



## Correlation between resource-generating powers of quantum gates

Aparajita Bhattacharyya, Ahana Ghoshal, and Ujjwal Sen 

*Harish-Chandra Research Institute, A CI of Homi Bhabha National Institute, Chhatnag Road, Jhansi, Prayagraj 211 019, India*

 (Received 31 December 2022; accepted 24 February 2023; published 7 March 2023)

We analyze the optimal basis for generating the maximum relative entropy of quantum coherence by an arbitrary gate on a two-qubit system. The optimal basis is not unique and the high-quantum-coherence-generating gates are also typically high-entanglement-generating ones and vice versa. However, the profile of the relative frequencies of Haar random unitaries generating different amounts of entanglement for a fixed amount of quantum coherence is different from the one in which the roles of entanglement and quantum coherence are reversed, although both follow a Beta distribution.

DOI: [10.1103/PhysRevA.107.032406](https://doi.org/10.1103/PhysRevA.107.032406)

### I. INTRODUCTION

The characterization of resource theory within quantum information science and technology was initiated with the theory of entanglement [1–4]. In general, a resource theory is constructed by putting certain natural constraints on the set of all quantum-mechanical operations to perform a specific job and the restrictions are overcome by utilizing certain resources. The nature of the constraints of course depends on the accessible physical system and the job at hand. In entanglement theory and practice, the restriction is set by the constraint that the observers, generally assumed to be at distant locations, will be able to perform only local quantum operations and classical communication and the resources are the entangled states shared by the same observers. In this manner, entanglement becomes useful in several interesting phenomena and tasks like quantum teleportation [5–7], quantum cryptography [8–10], and quantum dense coding [11,12]. Quantum coherence [13–16] (see also [17–19]) is also one of the principal resources in quantum phenomena and information tasks and along with being the reason for the classic interference phenomena it is also useful in jobs in quantum-enhanced metrology (see, e.g., [20–22]), quantum algorithms (see, e.g., [23–27]), quantum state discrimination (see, e.g., [28,29]), etc. The allowed operations are now the so-called incoherent operations and the resources are the quantum coherent states.

Quantifying the entanglement generated by quantum evolutions has been extensively studied in the literature (see, e.g., [30–50]). In particular, the two-qubit unitaries that generate maximal entanglement from zero-resource pure input states (i.e., two-qubit pure product states) were identified, among other things, in Ref. [31]. The effect of auxiliaries on the entanglement-generating ability was considered in, e.g., [31,35,41]. The case of mixed-state inputs was considered in, e.g., [32,34]. Generation of maximal entanglement using global unitaries of arbitrary bipartite dimensions was considered in, e.g., [43]. The asymptotic limit of the entanglement-generating capacity of a bidirectional channel acting on two  $d$ -dimensional systems has also been investigated in, e.g., [44]. The relation of entanglement generation

of two-qubit unitary operators with their distinguishability was uncovered in [46]. Reference [47] found two-qubit mixed states whose entanglement content cannot be increased by unitary transformations.

Similar to the path followed in entanglement theory, various aspects of the quantitative theory of quantum coherence have been uncovered [13–16]. In particular, different properties of the incoherent and coherence-generating operations have been identified and maximally coherent states have been analyzed. It is understood that interconnections exist between the resource theories of entanglement and quantum coherence. However, we recall that while entanglement is basis independent as long as we stick to local bases, quantum coherence is almost strictly basis dependent. Interrelations between the two resource theories have been studied in, e.g., [51–65]. In particular, given a global unitary operation on a bipartite system, an arbitrary unentangled input state does not generate entanglement. Also, defining quantum coherence with respect to local bases leads to a conceptualization of entanglement [60,65]. There have also been studies on interrelations between quantum coherence and other resources such as non-locality [66–68], non-Markovianity [69–74], and quantum discord [75–77]. Also, a relationship between classical communication and entanglement generation of two-qubit unitary operators was found in [78]. Reference [79] considered a thermal state and found the maximum amount of quantum coherence that can be generated when acted upon by a unitary operator. In [53] a basis-independent measure of quantum coherence was constructed and it was shown that it is equivalent to quantum discord. A quantum coherence-generating power for quantum channels, acting on incoherent states, was defined in [80]. The quantum-coherence-generating power of quantum dephasing processes was considered in [81]. Parallel to the concepts of distillable entanglement [82,83] and entanglement cost [82,84], quantum coherence distillation and quantum coherence cost were considered in [15].

In this paper we begin by exploring the maximal quantum-coherence-generating power of an arbitrary two-qubit unitary gate. The parallel case for maximal entanglement generation was considered in [31]. We provide a formal definition of the

power, which involves a maximum over all product bases of the underlying tensor-product Hilbert space. We define the same for arbitrary bases also.

We then compare the quantum coherence generation with entanglement generation for generic two-qubit unitaries. We find in particular that there exists a general tendency of a randomly chosen unitary to produce high quantum coherence when the entanglement generation is high and conversely to produce high entanglement when the quantum coherence generation is high. We make this statement more precise by considering relative frequencies of randomly chosen unitaries to fall in a chosen region on the entanglement-quantum coherence plane (with finite precision). These facts are represented in Figs. 3, 5, 7 below. We believe that this correlation between the different resource-generating powers for two-qubit unitaries is potentially useful for further analysis of resources and their generation within quantum technologies and also to lead to fundamental interrelations between these resources.

Furthermore, we analyze the relative frequency of a randomly generated unitary to have a certain entanglement and quantum-coherence-generating power (with finite precision). We find that the profiles of the relative frequencies for a fixed quantum-coherence-generating power and a fixed entanglement-generating one are qualitatively similar and follow a Beta distribution, but are quantitatively different.

Entanglement and quantum coherence are among the most important resources for quantum information tasks and we find that a unitary that generates maximum entanglement also generates maximum quantum coherence and vice versa. This fact may have fundamental as well as practical implications. On the practical front, this result may potentially imply that a quantum device implementing a task that necessarily requires high entanglement can with little effort be transformed into one implementing a different task which requires high quantum coherence and vice versa. More fundamentally, the result may indicate an underlying universality between entanglement and quantum coherence, in that devices creating a high amount of one create a high amount of the other with high probability.

The remainder of the paper is arranged as follows. The relevant information from previous literature is discussed in Sec. II. This includes the definition of entanglement-generating power and its evaluation for two-qubit unitary gates. We also present here a formal definition of the quantum-coherence-generating power of unitary gates. In Sec. III we present our results on the quantum-coherence-generating power of two-qubit unitaries. We compare the entanglement and quantum coherence generations of several paradigmatic two-qubit gates in Sec. IV. In Sec. V we consider the same comparison for Haar uniformly generated two-qubit unitaries. We present a summary in Sec. VI.

## II. PRELIMINARIES

We wish to deal with the resource-generating power of two-party unitaries, when the resource is either entanglement or quantum coherence. Let the two parties be Alice ( $A$ ) and Bob ( $B$ ), with the system they possess being defined on the Hilbert space  $\mathcal{H}_A \otimes \mathcal{H}_B$ .

The amount of entanglement generated by applying an arbitrary unitary operator  $U_{AB}$  is given by

$$E_g(U_{AB}) = \max_{\varrho_{AB}} [E(U_{AB}\varrho_{AB}U_{AB}^\dagger) - E(\varrho_{AB})], \quad (1)$$

where the maximization is over all states  $\varrho_{AB}$  on  $\mathcal{H}_A \otimes \mathcal{H}_B$  and  $E$  is a measure of entanglement for two-party quantum systems. One can also choose to consider the more general situation where the evolution acts on locally extended Hilbert spaces and an additional optimization is performed over all such extensions. For pure bipartite states, the local von Neumann entropy is a good measure of the state's entanglement [85], so we use

$$E(|\psi\rangle) = -\text{Tr}(\rho_A \log_2 \rho_A) = -\text{Tr}(\rho_B \log_2 \rho_B), \quad (2)$$

where  $\rho_A$  is the partial trace of  $|\psi\rangle\langle\psi|$  over the subsystem  $B$  and similarly for  $\rho_B$ . In this paper we restrict the study to pure input states and to input states having zero resource. Therefore, the input states are pure product states so that

$$E_g(U) = \max_{|\psi\rangle \otimes |\phi\rangle} S(\text{Tr}_{A/B} P[U_{AB}|\psi\rangle_A \otimes |\phi\rangle_B]), \quad (3)$$

where  $P[|\chi\rangle] = |\chi\rangle\langle\chi|$  and  $S(\sigma) = -\text{Tr}(\sigma \log_2 \sigma)$ . Moreover, we will restrict ourselves to two-qubit systems, for which the entanglement-generating power was considered in Ref. [31].

A conceptually different entanglement quantifier can be considered by using the Nielsen-Vidal entanglement monotones, which characterize transformations between bipartite pure states [86–90]. If  $|\psi\rangle$  is a pure state representing a bipartite quantum system corresponding to  $\mathbb{C}^n \otimes \mathbb{C}^n$ , then its Schmidt decomposition is given by

$$|\psi\rangle = \sum_{i=1}^n \sqrt{\alpha_i} |i_A i_B\rangle, \quad (4)$$

with  $\{\sqrt{\alpha_i}\}$  the Schmidt coefficients having  $\sum_{i=1}^n \alpha_i = 1$ , and we further assume that they are ordered as  $\alpha_i \geq \alpha_{i+1} \geq 0$ . Here  $\{|i_A\rangle\}$  and  $\{|i_B\rangle\}$  are the sets of eigenvectors of the reduced subsystems of  $|\psi\rangle$ , corresponding to the eigenvalues  $\alpha_i$ . A family of entanglement monotones  $E_k(|\psi\rangle)$  for a positive bipartite system, for  $k = 1, 2, \dots, n$ , can be defined as [87]

$$E_k(|\psi\rangle) = \sum_{i=k}^n \alpha_i. \quad (5)$$

So the amount of entanglement generated by applying an arbitrary unitary operator  $U_{AB}$ , by using  $E_k(|\psi\rangle)$  as a measure of entanglement, is given by

$$\bar{E}_g(U) = \max_{|\psi\rangle \otimes |\phi\rangle} E_k(U_{AB}|\psi\rangle_A \otimes |\phi\rangle_B). \quad (6)$$

Note that  $E_1$  is always unity. As we are concentrating on two-qubit systems, here  $k$  runs over 1 and 2. Therefore, for our purposes,  $k = 2$  in Eq. (6).

We now discuss quantum coherence generation by the unitary operator  $U_{AB}$ . To deal with this question, we first need to fix the basis with respect to which the quantum coherence is to be calculated. Let us suppose that this basis of  $\mathcal{H}_A \otimes \mathcal{H}_B$  is

$$\mathcal{B} = |\psi_i\rangle_{i=1}^{d_A d_B}, \quad (7)$$

where  $d_A = \dim \mathcal{H}_A$  and likewise for  $d_B$ . The coherence power [53,91], with respect to a basis  $\mathcal{B}$ , generated by the unitary  $U_{AB}$ , is given by

$$C_g(U_{AB}|\mathcal{B}) = \max_{\varrho_{AB}} [C(U_{AB}\varrho_{AB}U_{AB}^\dagger|\mathcal{B}) - C(\varrho_{AB}|\mathcal{B})], \quad (8)$$

where again, like in the case of entanglement generation, the maximization is over all states  $\varrho_{AB}$  on  $\mathcal{H}_A \otimes \mathcal{H}_B$ . Again, it is possible to consider the generating power by considering an additional optimization over all local extensions on Alice's and Bob's spaces. Here  $C$  is a measure of quantum coherence, and while several quantum coherence measures are known in the literature, we consider the relative entropy of quantum coherence and the  $l_1$ -norm of quantum coherence [14] for our purposes. Just like for the case of entanglement, we will consider pure inputs, so for relative entropy of coherence,

$$C(|\psi\rangle|\mathcal{B}) = S(\rho_{\text{diag}}), \quad (9)$$

where  $\rho_{\text{diag}}$  is a diagonal density matrix constructed by the diagonal elements of  $|\psi\rangle\langle\psi|$ , when written in the basis  $\mathcal{B}$ . We focus on product as well as arbitrary orthonormal bases of the bipartite system to compute the relative entropy of quantum coherence. Arbitrary product bases in general bipartite quantum systems are a relatively less understood concept. However, for two-qubit systems, all product orthonormal bases have been characterized [92] and they can be expressed as

$$|00\rangle, \quad |01\rangle, \quad |1\eta\rangle, \quad |1\eta^\perp\rangle. \quad (10)$$

In the computational basis,  $|\eta\rangle$  and  $|\eta^\perp\rangle$  can be written as  $|\eta\rangle = \cos(\theta/2)|0\rangle + e^{i\phi}\sin(\theta/2)|1\rangle$  and  $|\eta^\perp\rangle = -e^{-i\phi}\sin(\theta/2)|0\rangle + \cos(\theta/2)|1\rangle$ , where  $0 \leq \theta \leq \pi$  and  $0 \leq \phi < 2\pi$ . The elements for an arbitrary two-qubit product basis can be chosen, for our purposes, as in (10). Since we optimize over all input states of two qubits for a given unitary, we have the freedom of choosing an arbitrary basis as the computational basis on each local qubit space. Therefore, while the general two-qubit product basis is  $|\eta'\eta''\rangle$ ,  $|\eta'\eta''^\perp\rangle$ ,  $|\eta'^\perp\eta\rangle$ , and  $|\eta'^\perp\eta^\perp\rangle$ , we can use the mentioned freedom to choose  $|\eta'\rangle = |0\rangle$  and  $|\eta'^\perp\rangle = |1\rangle$  for the first qubit and  $|\eta''\rangle = |0\rangle$  and  $|\eta''^\perp\rangle = |1\rangle$  for the second qubit.

The construction of an arbitrary two-qubit basis, which would then contain entangled elements, in general, can be attained by applying a two-qubit arbitrary nonlocal unitary on the four elements of the computational basis  $\{|00\rangle, |01\rangle, |10\rangle, |11\rangle\}$ . The two-qubit unitary can be formed by using the prescription of [31,93], discussed below [see Eq. (16)]. When acted on by the unitary, the computational basis elements  $|00\rangle$ ,  $|01\rangle$ ,  $|10\rangle$ , and  $|11\rangle$  yield four states, which serve as the four elements of an arbitrary basis.

Just like for the case of entanglement generation, we consider only those inputs for which the resource is vanishing. As we have already mentioned, we only consider pure inputs. Therefore, for quantum coherence generation with respect to a product or arbitrary orthogonal basis  $\mathcal{B}_{\mathbb{C}^2 \otimes \mathbb{C}^2}$  on the two-qubit Hilbert space, the inputs can only be the four states of  $\mathcal{B}_{\mathbb{C}^2 \otimes \mathbb{C}^2}$ . So finally the amount of quantum coherence with respect to the basis  $\mathcal{B}_{\mathbb{C}^2 \otimes \mathbb{C}^2}$  that is generated by using the unitary  $U_{AB}$  is

given by

$$C_g(U|\mathcal{B}_{\mathbb{C}^2 \otimes \mathbb{C}^2}) = \max_i C(U_{AB}|\phi_i\rangle_{AB}|\mathcal{B}_{\mathbb{C}^2 \otimes \mathbb{C}^2}), \quad (11)$$

where  $\mathcal{B}_{\mathbb{C}^2 \otimes \mathbb{C}^2} = \{|\phi_i\rangle_{AB}\}_{i=1}^4$ . Now, to obtain the quantum-coherence-generating power of the unitary with respect to product bases, we have to take a maximization over arbitrary product bases of the  $\mathbb{C}^2 \otimes \mathbb{C}^2$  Hilbert space. So we have

$$C_g(U) = \max_{\text{product bases } \mathcal{B}_{\mathbb{C}^2 \otimes \mathbb{C}^2}} \max_i C(U_{AB}|\phi_i\rangle_{AB}|\mathcal{B}_{\mathbb{C}^2 \otimes \mathbb{C}^2}). \quad (12)$$

Similarly, to obtain the same for arbitrary bases, we have

$$C'_g(U) = \max_{\text{arbitrary bases } \mathcal{B}_{\mathbb{C}^2 \otimes \mathbb{C}^2}} \max_i C(U_{AB}|\phi_i\rangle_{AB}|\mathcal{B}_{\mathbb{C}^2 \otimes \mathbb{C}^2}). \quad (13)$$

The quantum-coherence-generating power, with any other measure of quantum coherence, can be defined similarly as in Eqs. (12) and (13), for product and arbitrary bases, respectively, with only the measure  $C$  being replaced by some other measure. A measure of quantum coherence that is conceptually different from the relative entropy of quantum coherence is the  $l_1$ -norm of quantum coherence, being defined, for an arbitrary state  $|\psi\rangle$  and a basis  $\mathcal{B}$ , as

$$C_{l_1}(|\psi\rangle|\mathcal{B}) = \sum_{\substack{i,j \\ i \neq j}} |\rho_{i,j}|. \quad (14)$$

This is the sum of moduli of the off-diagonal elements of the density matrix when written in the basis  $\mathcal{B}$ . Similarly as for the relative entropy of quantum coherence, we can, e.g., optimize over all product bases to obtain

$$\bar{C}_g(U) = \max_{\text{product bases } \mathcal{B}_{\mathbb{C}^2 \otimes \mathbb{C}^2}} \max_i C_{l_1}(U_{AB}|\phi_i\rangle_{AB}|\mathcal{B}_{\mathbb{C}^2 \otimes \mathbb{C}^2}). \quad (15)$$

Henceforth in this paper, we continue with local von Neumann entropy as the entanglement quantifier (for pure bipartite states) as in Eq. (2) and the relative entropy of quantum coherence as the quantifier of quantum coherence as in Eq. (9) (for pure states). We will change the quantifier in Sec. V C.

An arbitrary two-qubit unitary operator can be written in the form [31,93]

$$U_{AB} = U_A \otimes U_B U_d V_A \otimes V_B, \quad (16)$$

where  $U_A, V_A, U_B, V_B \in \text{U}(2)$ . Here  $U_A, U_B, V_A$ , and  $V_B$  are unitaries acting on the local subsystems and  $U_d$  is a nonlocal unitary on  $\mathbb{C}^2 \otimes \mathbb{C}^2$  having the form

$$U_d = \exp(-i\alpha_x \sigma_x \otimes \sigma_x - i\alpha_y \sigma_y \otimes \sigma_y - i\alpha_z \sigma_z \otimes \sigma_z), \quad (17)$$

where  $\alpha_x, \alpha_y$ , and  $\alpha_z$  are real numbers and  $\sigma_x, \sigma_y$ , and  $\sigma_z$  are the Pauli matrices. The relevant ranges for  $\alpha_x, \alpha_y$ , and  $\alpha_z$  may depend on the resource being generated, as we see below.

To obtain the maximum entanglement generated by a fixed unitary, we have to perform a maximization over input states. Since we are taking the input states as arbitrary pure product states, we can forget about  $V_A$  and  $V_B$ , because they will just rotate the space of product states into itself. Also, it is of no use, in this case, to apply  $U_A \otimes U_B$ , as local unitaries will keep the entanglement unchanged. So while generating entanglement by a two-qubit unitary, it is enough to only deal with  $U_d$ , as the amount of entanglement generated will not be affected by the four local unitaries. In Ref. [31] it was shown that

whenever  $\alpha_x + \alpha_y \geq \pi/4$  and  $\alpha_y + \alpha_z \leq \pi/4$ , there always exists an input state for which we get maximal entanglement at the output, and outside the region, dictated by the above inequalities, in the  $(\alpha_x, \alpha_y, \alpha_z)$  parameter space, the maximum entanglement is given by

$$E = H\left(\frac{1 + \sqrt{1 - \bar{C}^2}}{2}\right), \quad (18)$$

where  $H(\cdot)$  is the binary entropy function, with  $\bar{C}$  given by [94,95]

$$\bar{C} = \max_{k,l} |\sin(\lambda_k - \lambda_l)|, \quad (19)$$

where  $k$  and  $l$  go from 1 to 4 and

$$\begin{aligned} \lambda_1 &= \alpha_x - \alpha_y + \alpha_z, \\ \lambda_2 &= -\alpha_x + \alpha_y + \alpha_z, \\ \lambda_3 &= -\alpha_x - \alpha_y - \alpha_z, \\ \lambda_4 &= \alpha_x + \alpha_y - \alpha_z. \end{aligned} \quad (20)$$

It is enough to consider the parameter range  $\pi/4 \geq \alpha_x \geq \alpha_y \geq \alpha_z \geq 0$ , as the maximal entanglement generated is a periodic function in the  $(\alpha_x, \alpha_y, \alpha_z)$  parameter space and completes a full period in this range.

Considering now the case of maximal quantum coherence generation over product bases and with the unitary  $U_{AB}$ , we note that the product basis  $\{|\phi_i\rangle\}_i$  in Eq. (11) is taken to another product basis by  $V_A \otimes V_B$ , which will anyway be considered in the maximization over product bases in (12). This argument is essentially the same for arbitrary bases also. So, in (12), (13), and (15), we can ignore  $V_A \otimes V_B$ . The  $U_A \otimes U_B$  remains relevant throughout the quantum coherence part of this paper and of course  $U_d$  is relevant in both entanglement and quantum coherence parts. For the optimizations, we have used the algorithms of NLOPT [96].

### III. QUANTUM-COHERENCE-GENERATING POWER OF THE UNITARY GATE

In this section we try to find the maximum-coherence-generating powers of two-qubit unitary operators. The unitary is of the form

$$U_{AB} = U_A \otimes U_B U_d V_A \otimes V_B. \quad (21)$$

The  $U_d$  is referred to as the Cartan kernel part of the general two-qubit unitary gate. The entanglement power of the gate depends only on the Cartan kernel part of the unitary and is not altered due to the presence of the local unitaries. However, these local unitaries along with the Cartan kernel part play a role in the quantum coherence power of the unitary. We set  $W_1 = V_A, W_2 = V_B, W_3 = U_A$ , and  $W_4 = U_B$ , with  $W_k \in \text{SU}(2)$  for  $k = 1, 2, 3$ , and 4, represented as

$$W_k = \begin{pmatrix} \cos \frac{\theta_k}{2} e^{(i/2)(\psi_k + \phi_k)} & \sin \frac{\theta_k}{2} e^{-(i/2)(\psi_k - \phi_k)} \\ -\sin \frac{\theta_k}{2} e^{(i/2)(\psi_k - \phi_k)} & \cos \frac{\theta_k}{2} e^{-(i/2)(\psi_k + \phi_k)} \end{pmatrix}, \quad (22)$$

where  $\theta_k \in [0, \pi]$ ,  $\phi_k \in [0, 2\pi]$ , and  $\psi_k \in [0, 4\pi]$ . The form of the nonlocal unitary  $U_d$  remains the same as in Eq. (17). We choose an arbitrary product basis according to (10) and evaluate the expression for the relative entropy of quantum coherence which is generated by  $U_{AB}$  when acting on an incoherent pure two-qubit quantum state. The unitary  $U_{AB}$  of the form given in Eq. (21) can be expressed as

$$U_{AB} = \begin{pmatrix} r_3 & r_1 & m_3 & m_1 \\ r_7 & r_5 & m_7 & m_5 \\ r_4 & r_2 & m_4 & m_2 \\ r_8 & r_6 & m_8 & m_6 \end{pmatrix}. \quad (23)$$

We now calculate the relative entropy of quantum coherence for each of the states in the basis  $\{|00\rangle, |01\rangle, |1\eta\rangle, |1\eta^\perp\rangle\}$ . They are given by

$$\begin{aligned} \tilde{S}_i &= -|r_{5-2i}|^2 \log_2 |r_{5-2i}|^2 - |r_{9-2i}|^2 \log_2 |r_{9-2i}|^2 \\ &\quad - \left| r_{10-2i} \cos \frac{\theta}{2} - e^{i\phi} r_{2i-2(-1)^i} \sin \frac{\theta}{2} \right|^2 \\ &\quad \times \log_2 \left| r_{10-2i} \cos \frac{\theta}{2} - e^{i\phi} r_{2i-2(-1)^i} \sin \frac{\theta}{2} \right|^2 \\ &\quad - \left| r_{2i-2(-1)^i} \cos \frac{\theta}{2} + e^{-i\phi} r_{10-2i} \sin \frac{\theta}{2} \right|^2 \\ &\quad \times \log_2 \left| r_{2i-2(-1)^i} \cos \frac{\theta}{2} + e^{-i\phi} r_{10-2i} \sin \frac{\theta}{2} \right|^2 \end{aligned} \quad (24)$$

for  $i = 1, 2$ . For  $i = 3, 4$ , the corresponding expressions for quantum coherence are

$$\begin{aligned} \tilde{S}_i &= - \left| m_{9-2i} \cos \frac{\theta}{2} - (-1)^i e^{-(1)^i \phi} m_{2i-5} \sin \frac{\theta}{2} \right|^2 \log_2 \left| m_{9-2i} \cos \frac{\theta}{2} - (-1)^i e^{-(1)^i \phi} m_{2i-5} \sin \frac{\theta}{2} \right|^2 \\ &\quad \times \left| m_{13-2i} \cos \frac{\theta}{2} - (-1)^i e^{-(1)^i \phi} m_{2i-1} \sin \frac{\theta}{2} \right|^2 \log_2 \left| m_{13-2i} \cos \frac{\theta}{2} - (-1)^i e^{-(1)^i \phi} m_{2i-1} \sin \frac{\theta}{2} \right|^2 \\ &\quad \times \left| \frac{1}{4} \{ m_8 [ -(-1)^i + \cos \theta ] + e^{2i\phi} m_2 [ (-1)^i + \cos \theta ] - e^{i\phi} (m_4 - m_6) \sin \theta \} \right|^2 \\ &\quad \times \log_2 \left| \frac{1}{4} \{ m_8 [ -(-1)^i + \cos \theta ] + e^{2i\phi} m_2 [ (-1)^i + \cos \theta ] - e^{i\phi} (m_4 - m_6) \sin \theta \} \right|^2 \\ &\quad \times \left| \frac{1}{4} \{ e^{i\phi} [ -(-1)^i m_4 - (-1)^i m_6 + (m_4 - m_6) \cos \theta ] + (e^{2i\phi} m_2 + m_8) \sin \theta \} \right|^2 \\ &\quad \times \log_2 \left| \frac{1}{4} \{ e^{i\phi} [ -(-1)^i m_4 - (-1)^i m_6 + (m_4 - m_6) \cos \theta ] + (e^{2i\phi} m_2 + m_8) \sin \theta \} \right|^2. \end{aligned} \quad (25)$$



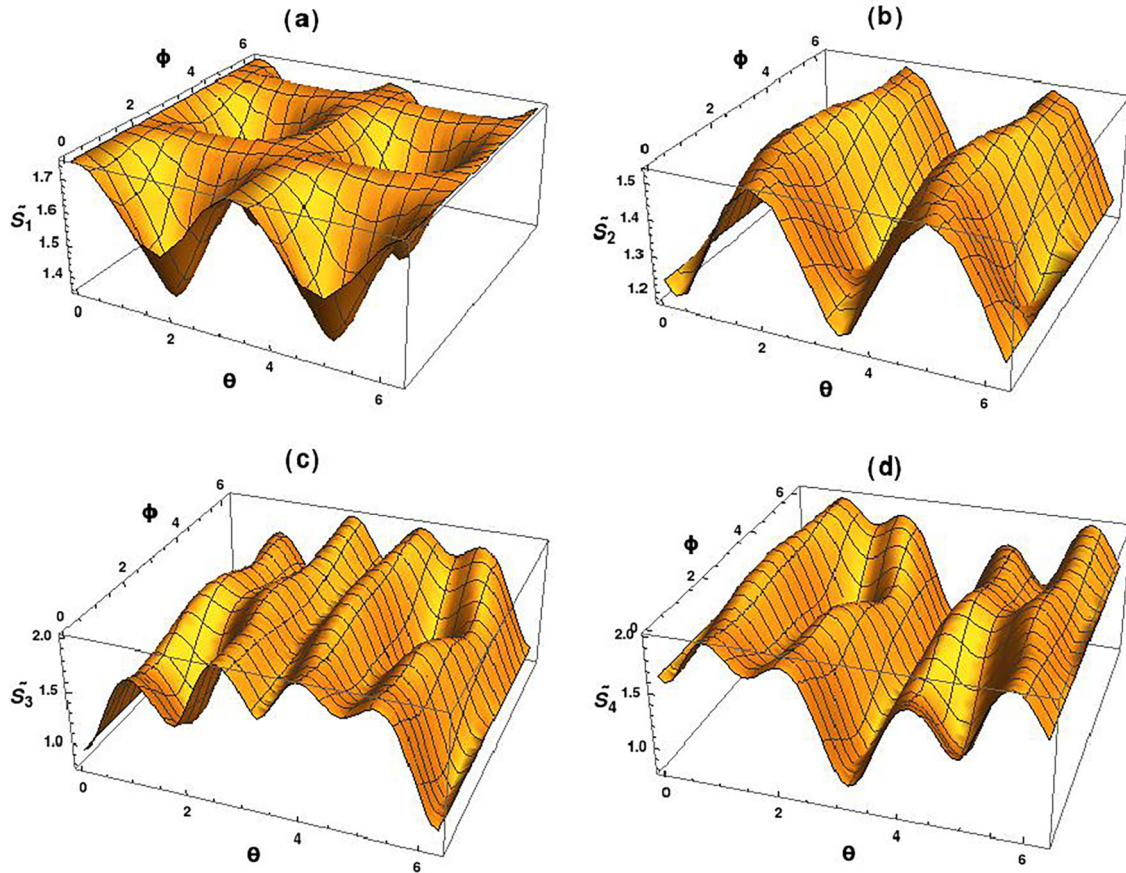


FIG. 1. Quantum coherence generation for a general two-qubit unitary. We plot here the relative entropy of quantum coherence that can be generated by the unitary  $U_{AB}$  as a function of the parameters of the product basis with respect to which the quantum coherence is defined and the elements of which act as initial states for the unitary evolution. The four plots are for the four elements of the product basis that act as the initial states of the evolution. The functions (a)  $\tilde{S}_1$ , (b)  $\tilde{S}_2$ , (c)  $\tilde{S}_3$ , and (d)  $\tilde{S}_4$  are plotted with respect to the basis parameters  $\theta$  and  $\phi$ . The fixed parameters of the unitary are taken as  $\alpha_x = 0.6078$ ,  $\alpha_y = 0.2625$ ,  $\alpha_z = 0.2287$ ,  $\theta_1 = 2.2330$ ,  $\phi_1 = 2.1630$ ,  $\psi_1 = 1.1980$ ,  $\theta_2 = 3.0700$ ,  $\phi_2 = 6.0630$ ,  $\psi_2 = 9.0910$ ,  $\theta_3 = 1.1000$ ,  $\phi_3 = 1.6570$ ,  $\psi_3 = 6.3530$ ,  $\theta_4 = 1.9190$ ,  $\phi_4 = 5.2110$ , and  $\psi_4 = 11.2600$ . The quantities  $\theta$  and  $\phi$  on the horizontal axes are presented in radians and the vertical axes are in bits. The  $\theta_i$ ,  $\phi_i$ , and  $\psi_i$ , for  $i = 1, 2, 3, 4$ , are in radians.

If we fix the unitary, i.e., if we fix all  $r_j$  and  $m_j$ , we can maximize these four functions with respect to  $\theta$  and  $\phi$ , the parameters of the product basis. Hence, following Eq. (11), the maximum quantum coherence for the fixed unitary and for the fixed basis is  $\max\{\tilde{S}_1, \tilde{S}_2, \tilde{S}_3, \tilde{S}_4\}$ , where the  $\tilde{S}_i$  for  $i = 1, 2$  are given in Eq. (24) and those for  $i = 3, 4$  are in (25). So, in accordance with Eq. (12), the maximum relative entropy of quantum coherence generated by the fixed unitary  $U_{AB}$  is given by

$$C_g(U_{AB}) = \max_{\theta, \phi} [\max\{\tilde{S}_1, \tilde{S}_2, \tilde{S}_3, \tilde{S}_4\}]. \quad (26)$$

All four functions  $\tilde{S}_i$  are periodic with respect to each of  $\alpha_x$ ,  $\alpha_y$ , and  $\alpha_z$  with a period of  $\pi$ . So, to evaluate the generation of relative entropy of quantum coherence, we can use the bounds  $\pi \geq \alpha_x, \alpha_y, \alpha_z \geq 0$  because beyond this region, the functions repeat their natures. In Fig. 1 we plot the four  $\tilde{S}_i$  with respect to the basis parameters for a fixed unitary. The numerical values of the parameters of the unitary considered here are given in the caption of Fig. 1. There are several maxima with respect to  $\theta$  in  $[0, \pi]$ . The last two functions

$\tilde{S}_3$  and  $\tilde{S}_4$  are neither periodic in  $\theta \in [0, \pi]$  nor symmetric around  $\theta = \pi$ . (The functions are of course periodic in  $\theta$  with a periodicity  $2\pi$ .) On the contrary,  $\tilde{S}_1$  and  $\tilde{S}_2$  are periodic in  $\theta \in [0, \pi]$ . It can be cumbersome to obtain the best choice of basis analytically, but it can be done numerically, using globally convergent routines. For a fixed unitary, we have observed numerically that the maximum quantum coherence corresponding to the initial states  $|00\rangle$  and  $|01\rangle$  (the maximum values of  $\tilde{S}_1$  and  $\tilde{S}_2$ ) are different, but for the states  $|1\eta\rangle$  and  $|1\eta^\perp\rangle$ , the maximum values of  $\tilde{S}_3$  and  $\tilde{S}_4$  are equal. Here, along with the possibility that the  $\tilde{\theta}_{m_i}$  and  $\tilde{\phi}_{m_i}$  are different for different  $i$ , each of the functions  $\tilde{S}_i$  can have multiple maxima in the parameter space of  $\theta$  in  $[0, \pi]$  and  $\phi$  in  $[0, 2\pi]$ . So we have that, for a general unitary, the best choice of basis for quantum coherence generation is not unique and the number of best bases can even be more than four. We have numerically observed that the four functions  $\tilde{S}_i$  are periodic in each of  $\alpha_x$ ,  $\alpha_y$ , and  $\alpha_z$  and considering the parameter range  $[0, \pi]$  for the  $\alpha$  is sufficient; we use this information for further analysis and illustration of the quantum coherence power of  $U_{AB}$ .

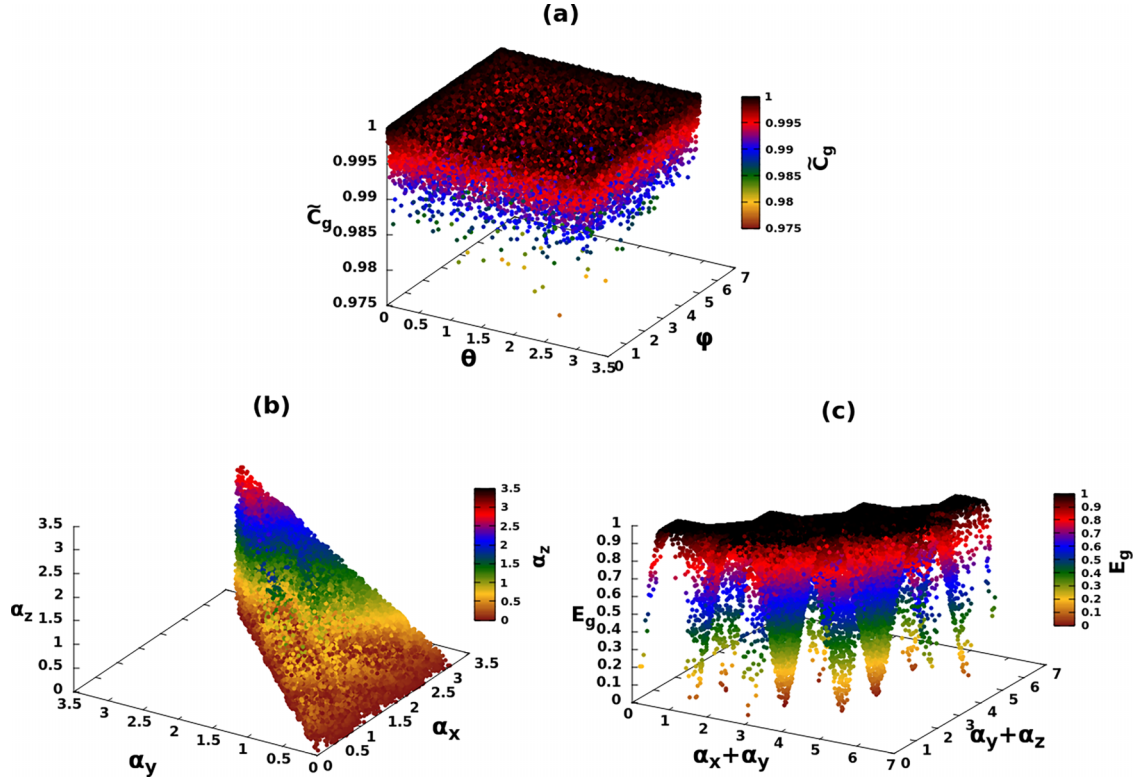


FIG. 2. Highest quantum coherences for maximal entanglement generating general two-qubit unitaries and vice versa. We investigate here the interplay between two resource-generating powers of the two-qubit unitaries  $U_{AB}$ . In (a) we generate  $2 \times 10^5$  unitaries which can create maximal entanglement and plot the maximal relative entropy of quantum coherence that can be generated by the same. The plot is depicted against a base of  $\theta$  along the  $x$  axis and  $\phi$  along the  $y$  axis, the parameters of the optimal basis for the quantum coherence generation. In (b), for  $2 \times 10^5$  points, we mark the region of the parameter space of the general two-qubit unitaries where the generated quantum coherence can reach the maximal value. In (c) the entanglement power of unitaries which can generate maximal quantum coherence are presented. For more details, see the text. The  $\theta$  and  $\phi$  axes are measured in radians. Here  $\alpha_x$ ,  $\alpha_y$ , and  $\alpha_z$  are dimensionless. The quantum coherence used in the plots is measured in bits and the entanglement therein are in ebits.

### A. Dependence of resource-generating power on parameters of $U_{AB}$

We try to compare here the two resource-generating powers (entanglement and quantum coherence) of the general unitary  $U_{AB}$ . As mentioned earlier, the local unitaries  $V_A$  and  $V_B$  have no contribution in the maximal creation of entanglement and they also do not affect the maximum generated quantum coherence. So here we perform the analysis and illustration by discarding the  $V_A \otimes V_B$  part and considering  $\tilde{U}_{AB} = U_A \otimes U_B U_d$  as equivalent to the whole unitary  $U_{AB}$ . In an actual experimental implementation, this can necessitate a local rotation of the optimal input state.

#### 1. Highest quantum coherence generated by $U_{AB}$ that allows maximal entanglement generation

We now find the maximum quantum coherence that can be generated by the unitary operators  $\tilde{U}_{AB}$ , which can maximize the entanglement of a bipartite quantum state to the maximal value, i.e., by those  $\tilde{U}_{AB}$  for which  $E_g(\tilde{U}_{AB}) = 1$ . Kraus and Cirac [31] showed that the maximal entanglement generated by a two-qubit unitary has certain periodicity and symmetry properties so that it is enough to consider the range  $\pi/4 \geq \alpha_x \geq \alpha_y \geq \alpha_z \geq 0$ . As previously discussed, the parameter

region is bounded by 0 to  $\pi$  in the case of evaluating the maximal quantum coherence generated and therefore this is the range that we use to numerically or analytically analyze quantum coherence generation or its interplay with entanglement generation. For this analysis, we first evaluate  $\tilde{U}_{AB}|\psi\rangle_A \otimes |\phi\rangle_B$  for arbitrarily chosen parameters of the unitary and then calculate the local von Neumann entropy of the output state and optimize over all  $|\psi\rangle_A, |\phi\rangle_B \in \mathbb{C}^2$ , where  $|\psi\rangle_A$  and  $|\phi\rangle_B$  are taken as

$$\begin{aligned} |\psi\rangle_A &= \cos(\bar{\alpha}/2)|0_A\rangle + e^{i\bar{\beta}} \sin(\bar{\alpha}/2)|1_A\rangle, \\ |\phi\rangle_B &= \cos(\bar{\gamma}/2)|0_B\rangle + e^{i\bar{\delta}} \sin(\bar{\gamma}/2)|1_B\rangle. \end{aligned} \quad (27)$$

Therefore, to find the best entanglement generation, the maximization will be over  $\bar{\alpha}, \bar{\gamma} \in [0, \pi]$  and  $\bar{\beta}, \bar{\delta} \in [0, 2\pi)$ , of  $S(\text{tr}_{A/B} P[\tilde{U}_{AB}|\psi\rangle_A \otimes |\phi\rangle_B])$ , for every set of values of the parameters  $\tilde{U}_{AB}$ , which are  $\alpha_x, \alpha_y, \alpha_z, \theta_i$ , and  $\phi_i$  and  $\psi_i$ , where  $i$  stands for 3 and 4. We choose  $2 \times 10^5$  unitaries in this parameter space, which can create maximal entanglement, and search for the maximum relative entropy of quantum coherence maximized over arbitrary pure product bases. The algorithm Direct-L [97] of NLOPT is used for the optimization. We get a finite probability of finding the maximal quantum coherence [see Fig. 2(a)]. The maximum value of the relative

entropy of quantum coherence for a two-qubit system is two bits, but here, for easy comparison with the maximal value of generated entanglement, we normalize the generated quantum coherence as

$$\tilde{C}_g(\tilde{U}_{AB}) = \frac{1}{2}C_g(\tilde{U}_{AB}), \quad (28)$$

and so we get the maximum quantum coherence equal to one bit instead of two bits. We recall that the maximal value of generated entanglement in a two-qubit system, according to the definition that we have used, is one unit of bipartite entanglement (ebit). It may be noted that instead of numerically optimizing entanglement with respect to the parameters of  $\tilde{U}_{AB}$  to identify the unitaries which can generate maximal entanglement, one can also decompose any arbitrary two-qubit unitary matrix  $U_{AB}$  into the form given in Eq. (21) following the procedure suggested in [31] and then the constraints on the parameters of the unitaries for generating  $E_g(U_{AB}) = 1$  can be used. However, to keep using the expressions for entanglement generation from Ref. [31], we must identify the rule for going from the bigger range of parameters to the smaller one. This is as follows.

We choose  $\alpha_i$ , where  $i$  can be  $x$ ,  $y$ , or  $z$ , in the range  $[0, \pi]$ . If we wish to find the maximal entanglement generated by the corresponding unitary, we set  $\tilde{\alpha}_i = \alpha_i$  if  $\alpha_i \leq \pi/4$  and  $\tilde{\alpha}_i = \pi/2 - \alpha_i$  if  $\pi/4 \leq \alpha_i \leq \pi/2$ , and using the symmetry of generated entanglement around  $\pi/4$ ,  $U_d(\{\tilde{\alpha}_i\})$  and  $U_d(\{\alpha_i\})$  generate the same entanglement. As previously mentioned, the local unitaries  $U_A$ ,  $U_B$ ,  $V_A$ , and  $V_B$  can be ignored in the case of entanglement generation. If  $\alpha_i \in [\pi/2, \pi]$ , we first use periodicity of the generated entanglement and go to an equivalent set of parameters  $\alpha'_i$ , equivalent with respect to entanglement generation, where  $\alpha'_i = \alpha_i - \pi/2$ . If  $\alpha'_i \in [0, \pi/4]$ , then we set  $\tilde{\alpha}_i = \alpha'_i$ , and if  $\alpha'_i \in [\pi/4, \pi/2]$ , then we use the symmetry of the entanglement generated and set  $\tilde{\alpha}_i = \pi/2 - \alpha'_i$ .

So now we have all the  $\tilde{\alpha}_i$  in the parameter range from 0 to  $\pi/4$ , but the order  $\alpha_x \geq \alpha_y \geq \alpha_z$ , which was present in the range 0 to  $\pi$ , may get altered in the case of  $\tilde{\alpha}_i$ , as the symmetry about  $\pi/4$  of generated entanglement is a reflection symmetry. Hence, the conditions  $\alpha_x + \alpha_y \geq \pi/4$  and  $\alpha_y + \alpha_z \leq \pi/4$  for obtaining maximal entanglement in the case when the  $\alpha_i$  belong to the range  $[0, \pi/4]$  have to be modified. Suppose that after the mapping we have the order  $\tilde{\alpha}_i \geq \tilde{\alpha}_j \geq \tilde{\alpha}_k$ , where  $i, j, k$  are from the set  $\{x, y, z\}$  and there are no repetitions. The conditions for getting maximal entanglement will then be  $\tilde{\alpha}_i + \tilde{\alpha}_j \geq \pi/4$  and  $\tilde{\alpha}_j + \tilde{\alpha}_k \leq \pi/4$ . Therefore, we have the  $\alpha_i$  in the parameter space 0 to  $\pi$ , which can generate maximal entanglement. Then we can analyze the maximal quantum coherence that can be generated by unitaries that can generate maximally entangled states.

## 2. Maximal-quantum-coherence-generating unitaries

We now try to identify the  $\alpha_x$ ,  $\alpha_y$ , and  $\alpha_z$ , corresponding to which we get  $\tilde{C}_g(\tilde{U}_{AB}) = 1$ , when the unitary operator  $\tilde{U}_{AB}$  acts on an incoherent two-qubit pure quantum state. In Fig. 2(b) we depict the region of the  $(\alpha_x, \alpha_y, \alpha_z)$  space for random choices of the remaining parameters (i.e.,  $\theta_j$ ,  $\phi_{j_2}$ , and  $\psi_j$  for  $j$  running over 3 and 4), at which the unitary  $\tilde{U}_{AB}$  can lead

to maximal quantum coherence (maximization using ISRES [98]).

## 3. Highest entanglement generated by $U_{AB}$ that allows maximal quantum-coherence generation

In Fig. 2(c) we look at the entanglement that can be generated by the unitaries which can generate maximum quantum coherence while operating on the set of two-qubit incoherent pure states. The unitaries are chosen from Fig. 2(b). We use the parameters  $\alpha_x + \alpha_y$  and  $\alpha_y + \alpha_z$  as axes of the base against which the generated entanglement is depicted. Note however that these  $\alpha_x$ ,  $\alpha_y$ , and  $\alpha_z$  belong to the range  $[0, \pi]$  and so for calculation of the maximal entanglement generation, we need to go to the range  $[0, \pi/4]$ . Since there is a reflection symmetry that is used in the transformation between the two ranges, the ordering between the  $\alpha$ 's is lost. Consequently, the condition for reaching maximal entanglement from Ref. [31] cannot be used directly in the presentation in Fig. 2(c). In Fig. 2(c) we find a finite probability of points (representing unitaries) for which the generated entanglement is one ebit. From Figs. 2(a) and 2(c) we can conclude that unitaries exist for which both entanglement and quantum coherence generations are maximal.

## IV. RESOURCE-GENERATING POWERS OF PARADIGMATIC QUANTUM GATES

We choose here a few paradigmatic two-qubit gates that are widely used in quantum device circuits and compare their entanglement and quantum coherence power. For completeness, we first define the gates and then present a table containing the powers.

Arguably, the most well-known two-qubit gate is the controlled-NOT (CNOT) operator. The NOT gate is the same as the Pauli  $\sigma_x$  operator. The CNOT operator is defined on the two-qubit space as  $U_{\text{CNOT}} = |0\rangle\langle 0| \otimes I_2 + |1\rangle\langle 1| \otimes \sigma_x$ , where  $I_2$  is the identity operator on the qubit space. The CNOT is therefore the controlled- $\sigma_x$  operator. Similarly, one can consider the controlled- $\sigma_z$  operator as  $U_{\text{CZ}} = |0\rangle\langle 0| \otimes I_2 + |1\rangle\langle 1| \otimes \sigma_z$ , which is usually referred to as the CZ gate. The SWAP gate is a two-qubit linear operator defined as  $U_{\text{SWAP}}|\psi\rangle|\phi\rangle = |\phi\rangle|\psi\rangle$ , where  $|\psi\rangle, |\phi\rangle \in \mathbb{C}^2$ . (One can of course define a SWAP gate in arbitrary bipartite dimensions  $\mathbb{C}^d \otimes \mathbb{C}^d$ .) The SWAP gate of course cannot create any entanglement by acting on a product state. The situation is very different for its square root, for which the matrix representation in the computational basis is

$$U_{\sqrt{\text{SWAP}}} = \begin{pmatrix} 1 & 0 & 0 & 0 \\ 0 & \frac{1}{2}(1+i) & \frac{1}{2}(1-i) & 0 \\ 0 & \frac{1}{2}(1-i) & \frac{1}{2}(1+i) & 0 \\ 0 & 0 & 0 & 1 \end{pmatrix}. \quad (29)$$

So far, we have not considered any product unitaries (i.e., product of two single-qubit unitaries), which trivially have vanishing entanglement power. They however can have non-trivial quantum coherence power. We consider three such product unitary gates. The first one that we choose is  $U_{\text{YX}} = \sigma_y \otimes \sigma_x$ . One can of course consider any other combination of the Pauli spin- $\frac{1}{2}$  operators. An important single-qubit unitary



TABLE I. Powers of entanglement and quantum coherence generation for unitaries discussed in Sec. IV, correct to four significant figures.

Gate ( $U$ )	$E_g(U)$	$\tilde{C}_g(U)$
CNOT	1	0.5
CZ	1	0.5
SWAP	0	0.7768
$\sqrt{\text{SWAP}}$	1	0.75
YX	0	0.5
$H \otimes H$	0	1
$H \otimes I_2$	0	0.75

that is almost universally present in a quantum algorithm circuit is the Hadamard gate, defined by  $H|0\rangle = \frac{1}{\sqrt{2}}(|0\rangle + |1\rangle)$  and  $H|1\rangle = \frac{1}{\sqrt{2}}(|0\rangle - |1\rangle)$ , supplemented by linearity. The other two product unitaries that we consider are  $H \otimes H$  and  $H \otimes I_2$ . In Table I we present the powers of entanglement and quantum coherence generation for the above unitaries, correct to four significant figures.

In the succeeding section, we look at Haar uniformly generated random two-qubit unitaries and compare their entanglement and quantum coherence powers.

## V. RESOURCE-GENERATING POWERS OF HAAR RANDOM QUANTUM GATES

In this section we compare the entanglement and quantum-coherence-generating powers of Haar uniformly generated gates on two-qubit systems. The Haar uniform generation is effected by using the Ginibre ensemble [99]. For each unitary, we numerically evaluate the  $E_g$  by optimizing over arbitrary two-qubit pure product states as inputs [Eq. (27)]. For the same unitary, we also obtain  $\tilde{C}_g$  for a pure incoherent input state and optimize over the inputs as well as the product (10) or arbitrary bases, with respect to which the quantum coherence is defined. The two maximizations are done independently so that the input state for which the maximum entanglement is attained can be different from the state for which we obtain the maximum quantum coherence. Instead of numerically maximizing the entanglement for a unitary, one can also use the canonical decomposition given in [31]. We present our observations on the resource-generating powers of Haar uniformly generated unitaries in the next three subsections. The first two contain discussions using the measures of entanglement and coherence as the local von Neumann entropy and the relative entropy of coherence, respectively. In the third one, we illustrate the results of our investigations, considering the Nielsen-Vidal monotone and  $l_1$ -norm of coherence, defined in Eqs. (6) and (15), respectively, as measures of the corresponding resources.

### A. Maximal entanglement vs maximal quantum coherence in product bases

In Fig. 3 we depict  $E_g$  and  $\tilde{C}_g$  on the base axes and  $\nu$ , the relative frequency of the number of unitaries generating the corresponding  $E_g$  and  $\tilde{C}_g$ , plotted along the vertical axis. Of course, finite precision is needed to calculate the relative fre-

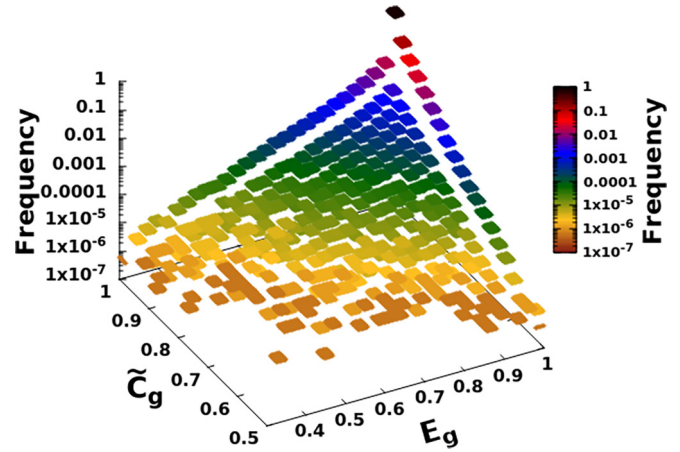


FIG. 3. Resource-generating tendencies of Haar random two-qubit unitaries. We Haar uniformly generate a large number of two-qubit unitaries and find their entanglement and quantum coherence power. We then divide the  $(E_g, \tilde{C}_g)$  space into small squares and find the relative frequencies of the number of unitaries that fall in those squares. These relative frequencies are plotted along the vertical axis, which is on a logarithmic scale. The quantity plotted on the vertical axis is dimensionless, while  $E_g$  and  $\tilde{C}_g$  are in ebits and bits, respectively. See the text for more details.

quencies, and we have a total of  $1.6 \times 10^3$  squares, each being of area  $2.5 \times 10^{-2}$  ebits  $\times$   $2.5 \times 10^{-2}$  bits on the entanglement-quantum coherence plane. We generate a total of  $1.6 \times 10^6$  two-qubit unitaries, Haar uniformly, and for each square we plot (on the vertical axis) the relative frequency of the number of unitaries having the ability to generate the numerical values of resources in ebits and bits corresponding to that square.

This depiction describes how the relative frequency increases progressively from approximately zero to approximately one, as we go along the plane in the direction of increasing entanglement and increasing quantum coherence, and reaches a peak value at the point where entanglement and quantum coherence are both maximal. Note that the vertical axis has a logarithmic scale in the depiction and this implies that there is a large fraction of unitaries, in the space of two-qubit unitaries, for which both entanglement and quantum coherence generation are nearly maximal.

In Fig. 4(a) we focus attention on the high-entanglement end of Fig. 3. Precisely, we have restricted the entanglement range to  $[0.9775, 1]$  in ebits. Similarly, Fig. 4(b) depicts the same in the high-quantum coherence range  $[0.9775, 1]$  in bits. We find that there is asymmetry between the entanglement and quantum coherence generations, near their respective maximal values.

In Figs. 4(c) and 4(d) we look at both resources by first fixing the other resource at a fixed value. Precisely, we take the fixed values to be the maximal ones in both cases. In Fig. 4(c) the fixed resource is entanglement, while in Fig. 4(d) it is quantum coherence. The asymmetric nature between entanglement and quantum coherence generation, as seen in the relative frequencies of Haar random unitaries, that we had mentioned before is now visible more clearly. We find that the numerically generated red circles in Figs. 4(c) and 4(d) can be well described by the Beta distribution, suitably scaled and



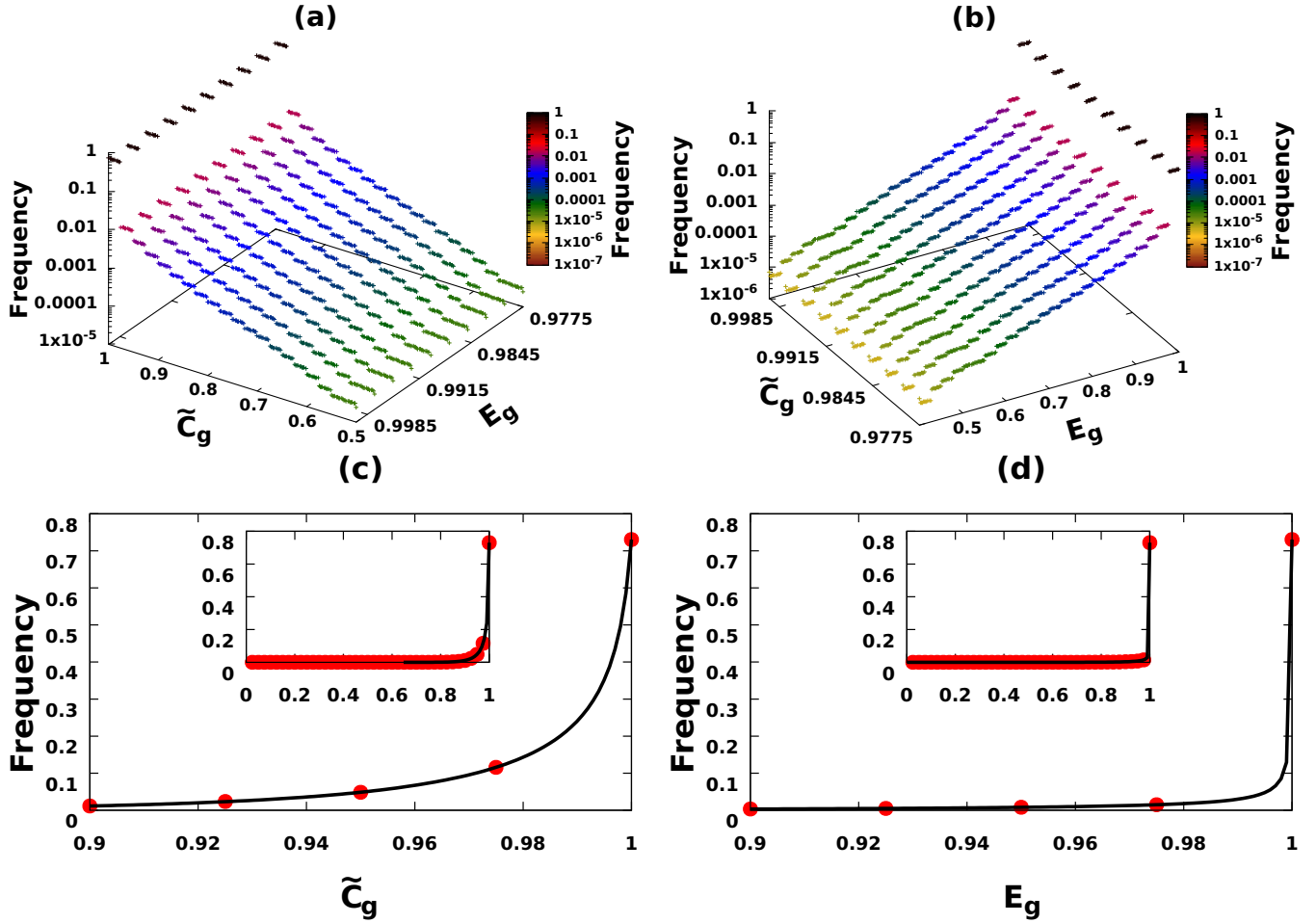


FIG. 4. Asymmetrical nature of resource-generating powers of two-qubit unitaries. (a) Magnified view of the plot in Fig. 3 when restricted to the range  $[0.9775, 1]$  on the entanglement axis. (b) Same as in (a) but for quantum coherence. The vertical axes are again in logarithmic scale in both (a) and (b). Just one cross section of the surface in (a) is analyzed in (c). The chosen cross section is for  $E_g = 1$ . The inset and the main plot in (c) differ only in the range of the horizontal axis. Also note that the vertical axis is in the normal scale in (c). The analysis in (d) is exactly the same as in (c) but with the roles of entanglement and quantum coherence reversed. The quantity plotted on the vertical axes is dimensionless, while on the horizontal axes  $E_g$  is in ebits and  $\tilde{C}_g$  is in bits. See the text for more details.

shifted; however, the parameters of the Beta distributions that fit the two cases are different. The fitting function therefore has the form

$$f_B(x) = dB(x; \alpha_B, \beta_B) + h \quad (30)$$

for  $x \in [0, 1]$ ,  $\alpha_B > 0$ , and  $\beta_B > 0$ . The explicit form of the Beta distribution  $B(x; \alpha_B, \beta_B)$  is given in the Appendix. For Fig. 4(c), the best-fit values of the exponents of  $f_B(x)$  are

$$\begin{aligned} \alpha_B &= 21.0539(\pm 1.244), \\ \beta_B &= 0.4694(\pm 3.057), \end{aligned} \quad (31)$$

with error equal to  $1.85 \times 10^{-4}$ . The numbers in parentheses indicate the respective 95% confidence intervals and the error mentioned is the minimum  $\chi^2$  error. The same numbers in Fig. 4(d) are

$$\begin{aligned} \alpha_B &= 9.1513(\pm 0.1627), \\ \beta_B &= 0.3766(\pm 0.0097), \end{aligned} \quad (32)$$

with error equal to  $1.186 \times 10^{-3}$ . (See the Appendix for the values of the other parameters.) We have used nonlinear least-squares fitting to obtain the values of the parameters, their 95% confidence intervals, and the error estimates for the fitting curves [100].

### B. Maximal entanglement vs maximal quantum coherence in arbitrary bases

Figure 5 depicts  $\tilde{C}'_g$  with  $E_g$  as a scatter plot. Here  $\tilde{C}'_g$  is just the normalized version of  $C'_g$ :  $\tilde{C}'_g(U_{AB}) = \frac{1}{2}C'_g(U_{AB})$ . The choice of zero-resource inputs and the methods of optimization are the same as in the preceding case of arbitrary product bases. Just like the preceding case, here also we observe the tendency of unitary gates to produce maximal entanglement along with maximal coherence. Most of the points of the scatter plot, depicted for  $16 \times 10^5$  Haar uniformly generated two-qubit unitaries, are concentrated near the region having both coherence and entanglement close to unity with a higher

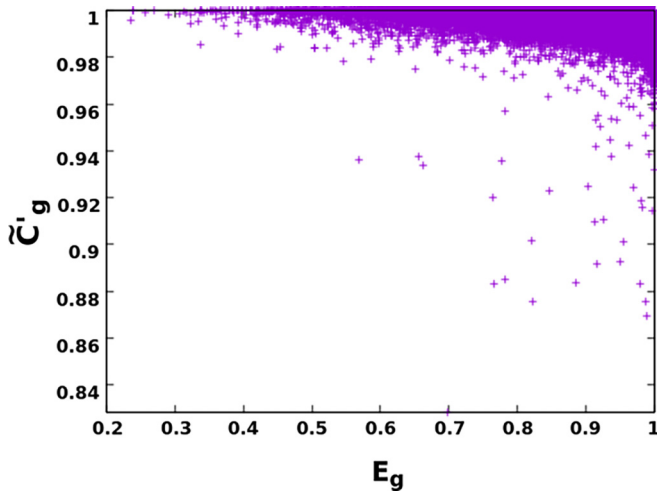


FIG. 5. Resource-generating power of Haar random two-qubit unitaries. Here we demonstrate a scatter plot of the maximum coherence  $\tilde{C}'_g$  vs maximum entanglement  $E_g$  by generating  $16 \times 10^5$  two-qubit unitaries Haar uniformly. Among the quantities plotted here,  $E_g$  is in ebits and  $\tilde{C}'_g$  is in bits.

spread along the entanglement axis. We can observe that the majority of unitaries produce  $\tilde{C}'_g$  approximately greater than or equal to 0.96 and there exist a finite probability to generate  $\tilde{C}'_g$  from 0.84 to 0.96. Typically, there appears almost no possibility to generate  $\tilde{C}'_g < 0.84$ .

We now depict the relative frequency of the number of unitaries generating  $E_g$  and  $\tilde{C}'_g$ , with the corresponding  $E_g$  and  $\tilde{C}'_g$  along the base axes in Fig. 6(a), in a manner similar to that in Fig. 4(b). We can see that the nature of the frequency in the former is qualitatively similar to that in the latter, with a progressively increasing frequency from approximately zero to one, reaching the maximum at  $E_g = 1$ . In Fig. 6(b) we plot

a cross section of Fig. 6(a) at  $C'_g = 1$ , and in this case also, the relative frequency exhibits a nature which can be fitted with the Beta function given in Eq. (30). The best-fit values for the parameters of  $f_B(x)$  and their corresponding 95% confidence intervals are provided in the Appendix.

### C. Examining the correlation between resource-generating powers for altered measures

We now discuss the resource-generating powers of Haar random quantum gates using an altered pair of measures of the resources. Here we use a Nielsen-Vidal entanglement monotone and the  $l_1$ -norm of quantum coherence as measures of entanglement and quantum coherence, respectively. The respective resource generating powers  $\tilde{E}_g$  and  $\tilde{C}_g$ , given in Eqs. (6) and (15), respectively, are presented in a scatter plot in Fig. 7 for  $13.5 \times 10^5$  Haar random unitaries. Like in previous investigations, here also most of the unitaries generate maximum maximum entanglement and maximum coherence. Along the coherence axis, the spread dies out after 0.4 bits, while along the entanglement axis, the spread is very small and most of the points are concentrated between  $1-10^{-5}$  and 1. Hence, in this scenario also, the maximum entanglement-generating unitaries are the maximum coherence-generating ones and vice versa.

## VI. CONCLUSION

There are two main themes of this paper. The first is to find the maximum quantum coherence that can be generated by two-qubit unitary gates from pure incoherent states and the second is to compare this generation with entanglement generation for the same gate from pure unentangled states, for generic two-qubit unitary gates.

With respect to the first theme, we dealt with the maximum quantum coherence generated by a general two-qubit

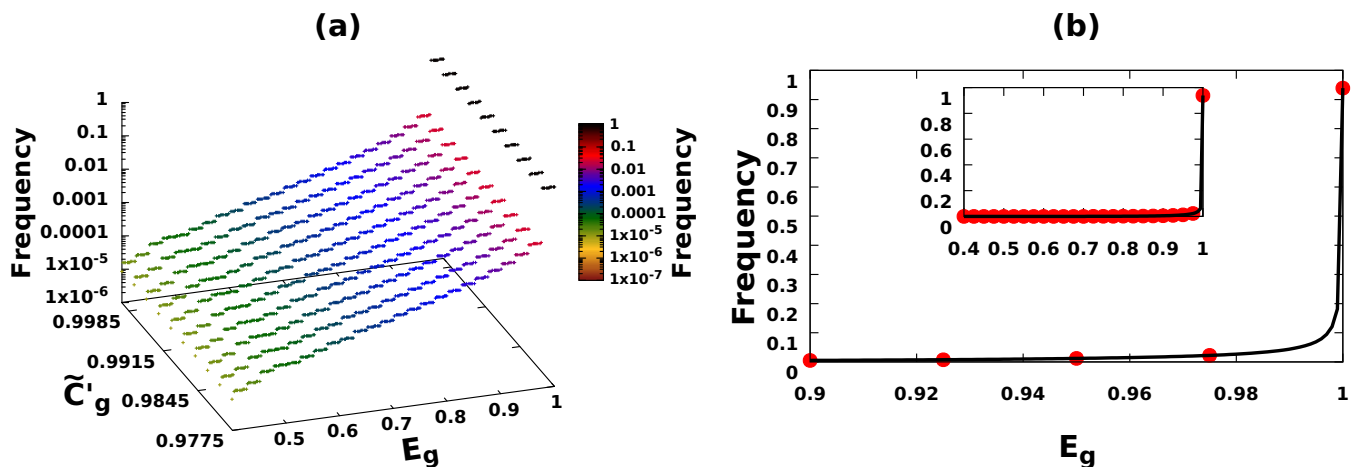


FIG. 6. Relative frequency vs the two resources generated by the Haar uniform random unitaries, where the optimum coherence is obtained by maximizing over all bases. (a) Relative frequency plotted in the range  $[0.9975, 1]$  on the coherence axis. (b) One cross section of (a) for  $\tilde{C}'_g = 1$ . All other considerations are the same as in Fig. 4. The quantities  $E_g$  and  $\tilde{C}'_g$  are expressed in ebits and bits, respectively, on the horizontal axes and the quantity represented on the vertical axis is dimensionless.

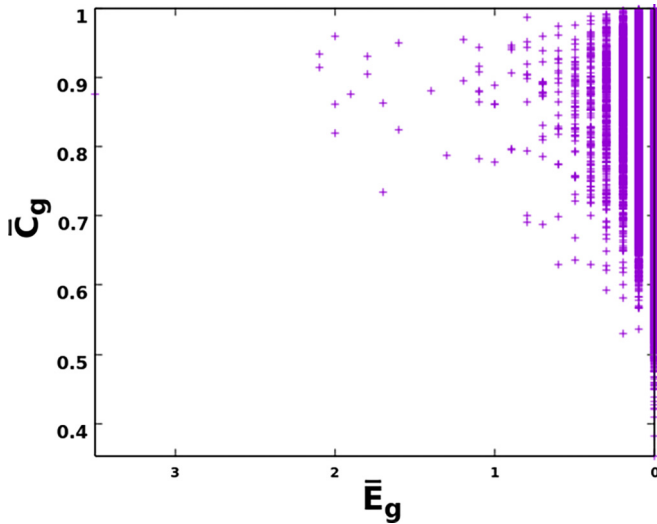


FIG. 7. Maximum coherence vs maximum entanglement generating power, defined by Eqs. (6) and (15), generated by Haar uniform random unitaries. Here  $\bar{C}_g$  is presented with respect to  $\bar{E}_g$  for  $13.5 \times 10^5$  Haar uniformly chosen two-qubit unitaries. The quantity plotted along the horizontal axis is in ebits and the one along the vertical axis is in bits. Along the horizontal axis,  $k$  represents  $1 - k \times 10^{-5}$  for  $k = 0, \dots, 3$ .

unitary operator acting on an incoherent pure state of an arbitrary product basis of two qubits and also a generic basis of the same. We discussed the best choice of basis to obtain the maximum coherence for a fixed unitary and the nature of the quantum coherences generated by the unitary when acting on different elements of the basis. The work of Kraus and Cirac [31] considered the parallel problem for entanglement generation and identified a class of two-qubit unitaries, which they called nonlocal unitaries. The same was referred to as the Cartan kernel part in the work of Khaneja and Glaser [93]. It is this part of the whole unitary that is responsible for entanglement generation, provided there is a certain arbitrariness present in the input. We performed the analysis for the general two-qubit unitaries, as even local unitaries can generate quantum coherence. We also analyzed the quantum-coherence-generating powers of unitaries that can create maximal entanglement and in parallel the entanglement power of maximally quantum-coherence-generating unitaries.

Finally, for the second theme, we considered the correlation between entanglement and quantum coherence generation for a generic two-qubit unitary gate, which we generated Haar uniformly by using the Ginibre ensemble. We found that the high-entanglement-generating unitaries are also typically high-quantum-coherence-generating ones and, conversely, the unitaries that generate high quantum coherence also typically generate high entanglement. It should be noted, however, that there is an inherent asymmetry between the entanglement and quantum-coherence generations. In particular, we analyzed the profile of the relative frequency of unitaries that can generate maximal entanglement to have the ability to create a given amount of quantum coherence and found that it can be well described by the Beta distribution. Role

reversal between entanglement and quantum coherence leads one to obtain a steeper curve, but still describable by the Beta distribution, albeit with a different set of distribution parameters.

Relations between different resource theories may help us understand a general structure among resource theories in quantum systems. Entanglement and quantum coherence are ubiquitous resources in quantum technologies. The connection uncovered here between entanglement and quantum-coherence generation for generic two-qubit global unitaries can potentially lead to fundamental interrelations between these resources and also to fresh applications and towards optimized usage of these resources in quantum devices. The interrelations between different resources of the same quantum device could potentially be of fundamental importance in utilizing these resources in an optimal way. A device that is known to be significantly good for generating a certain resource may not be so for generating another. We show however that the two quintessential quantum resources, viz., entanglement and quantum coherence, are related, and once we know that a device can generate a significant amount of entanglement, then we can be sure, with high probability, that the same can generate a significant amount of quantum coherence and vice versa.

#### ACKNOWLEDGMENTS

We acknowledge computations performed using ARMADILLO [101,102], NLOPT [96] (Direct-L [97], ISRES [98], and Cobyla [103]), and QICLIB [104] on the cluster computing facility of the Harish-Chandra Research Institute, India. We also acknowledge partial support from the Department of Science and Technology, Government of India, through QuEST (Grant No. DST/ICPS/QUST/Theme-3/2019/120).

#### APPENDIX: BETA DISTRIBUTION AND FITTING PARAMETERS FOR FIGS. 4(c), 4(d), AND 6(b)

The Beta distribution is a probability density function given by

$$B(x; \alpha_B, \beta_B) = \frac{\Gamma(\alpha_B + \beta_B)}{\Gamma(\alpha_B)\Gamma(\beta_B)} (x - x_0)^{\alpha_B - 1} [1 - (x - x_0)]^{\beta_B - 1} \quad (\text{A1})$$

for  $x \in [0, 1]$ ,  $\alpha_B > 0$ , and  $\beta_B > 0$ . Here  $x_0$  is a real number. For Fig. 4(c) the best-fit values of the parameters of  $f_B(x)$  and their respective 95% confidence intervals, within the nonlinear least-squares fit method, are

$$\begin{aligned} \alpha_B &= 21.0539(\pm 0.2618), \\ \beta_B &= 0.4694(\pm 0.0143), \\ d &= 0.0135(\pm 0.0003), \\ x_0 &= 0.0022(\pm 0.0001), \\ h &= -8.0159 \times 10^{-6}(\pm 1.793 \times 10^{-5}). \end{aligned} \quad (\text{A2})$$



The values of the same parameters in Fig. 4(d) are

$$\begin{aligned}\alpha_B &= 9.1513(\pm 0.1627), \\ \beta_B &= 0.3766(\pm 0.0097), \\ d &= 0.0019(\pm 3.049 \times 10^{-5}), \\ x_0 &= 6.8175 \times 10^{-5}(\pm 5.969 \times 10^{-6}), \\ h &= 9.6372 \times 10^{-6}(\pm 5.78 \times 10^{-6}).\end{aligned}\quad (\text{A3})$$

The following are the values of the same parameters in Fig. 6(b):

$$\begin{aligned}\alpha_B &= 8.9527(\pm 0.1871), \\ \beta_B &= 0.3949(\pm 0.0106), \\ d &= 0.0028(\pm 4.656 \times 10^{-5}), \\ x_0 &= 7.2652 \times 10^{-5}(\pm 7.066 \times 10^{-6}), \\ h &= 5.0638 \times 10^{-5}(\pm 1.506 \times 10^{-5}).\end{aligned}\quad (\text{A4})$$

- 
- [1] M. B. Plenio and S. Virmani, An introduction to entanglement measures, *Quantum Inf. Comput.* **7**, 1 (2007).
- [2] R. Horodecki, P. Horodecki, M. Horodecki, and K. Horodecki, Quantum entanglement, *Rev. Mod. Phys.* **81**, 865 (2009).
- [3] O. Gühne and G. Tóth, Entanglement detection, *Phys. Rep.* **474**, 1 (2009).
- [4] S. Das, T. Chanda, M. Lewenstein, A. Sanpera, A. Sen(De), and U. Sen, in *Quantum Information*, edited by D. Bruß and G. Leuchs (Wiley, Weinheim, 2019), Chap. 8.
- [5] C. H. Bennett, G. Brassard, C. Crépeau, R. Jozsa, A. Peres, and W. K. Wootters, Teleporting an Unknown Quantum State via Dual Classical and Einstein-Podolsky-Rosen Channels, *Phys. Rev. Lett.* **70**, 1895 (1993).
- [6] S. Pirandola, J. Eisert, C. Weedbrook, A. Furusawa, and S. L. Braunstein, Advances in quantum teleportation, *Nat. Photon.* **9**, 641 (2015).
- [7] T. Liu, The applications and challenges of quantum teleportation, *J. Phys.: Conf. Ser.* **1634**, 012089 (2020).
- [8] N. Gisin, G. Ribordy, W. Tittel, and H. Zbinden, Quantum cryptography, *Rev. Mod. Phys.* **74**, 145 (2002).
- [9] S. Pirandola, U. L. Andersen, L. Banchi, M. Berta, D. Bunandar, R. Colbeck, D. Englund, T. Gehring, C. Lupo, C. Ottaviani, J. Pereira, M. Razavi, J. S. Shaari, M. Tomamichel, V. C. Usenko, G. Vallone, P. Villoresi, and P. Wallden, Advances in quantum cryptography, *Adv. Opt. Photon.* **12**, 1012 (2020).
- [10] C. Portmann and R. Renner, Security in quantum cryptography, *Rev. Mod. Phys.* **94**, 025008 (2022).
- [11] C. H. Bennett and S. J. Wiesner, Communication via One- and Two-Particle Operators on Einstein-Podolsky-Rosen States, *Phys. Rev. Lett.* **69**, 2881 (1992).
- [12] Y. Guo, B. H. Liu, C. F. Li, and G. C. Guo, Advances in quantum dense coding, *Adv. Quantum Technol.* **2**, 1900011 (2019).
- [13] J. Åberg, Quantifying superposition, [arXiv:quant-ph/0612146](https://arxiv.org/abs/quant-ph/0612146).
- [14] T. Baumgratz, M. Cramer, and M. B. Plenio, Quantifying Coherence, *Phys. Rev. Lett.* **113**, 140401 (2014).
- [15] A. Winter and D. Yang, Operational Resource Theory of Coherence, *Phys. Rev. Lett.* **116**, 120404 (2016).
- [16] A. Streltsov, G. Adesso, and M. B. Plenio, Quantum coherence as a resource, *Rev. Mod. Phys.* **89**, 041003 (2017).
- [17] T. Theurer, N. Killoran, D. Egloff, and M. B. Plenio, Resource Theory of Superposition, *Phys. Rev. Lett.* **119**, 230401 (2017); S. Das, C. Mukhopadhyay, S. S. Roy, S. Bhattacharya, A. Sen (De), and U. Sen, Wave-particle duality employing quantum coherence in superposition with non-orthogonal pointers, *J. Phys. A: Math. Theor.* **53**, 115301 (2020).
- [18] C. Srivastava, S. Das, and U. Sen, Resource theory of quantum coherence with probabilistically non-distinguishable pointers and corresponding wave-particle duality, *Phys. Rev. A* **103**, 022417 (2021).
- [19] I. Banerjee, K. Sen, C. Srivastava, and U. Sen, Quantum coherence with incomplete set of pointers and corresponding wave-particle duality, [arXiv:2108.05849](https://arxiv.org/abs/2108.05849).
- [20] D. P. Pires, I. A. Silva, E. R. de Azevedo, D. O. Soares-Pinto, and J. G. Filgueiras, Coherence orders, decoherence and quantum metrology, *Phys. Rev. A* **98**, 032101 (2018).
- [21] A. Castellini, R. Lo Franco, L. Lami, A. Winter, G. Adesso, and G. Compagno, Indistinguishability-enabled coherence for quantum metrology, *Phys. Rev. A* **100**, 012308 (2019).
- [22] C. Zhang, T. R. Bromley, Y.-F. Huang, H. Cao, W.-M. Lv, B.-H. Liu, C.-F. Li, G.-C. Guo, M. Cianciaruso, and G. Adesso, Demonstrating Quantum Coherence and Metrology that is Resilient to Transversal Noise, *Phys. Rev. Lett.* **123**, 180504 (2019).
- [23] M. Hillery, Coherence as a resource in decision problems: The Deutsch-Jozsa algorithm and a variation, *Phys. Rev. A* **93**, 012111 (2016).
- [24] N. Anand and A. K. Pati, Coherence and entanglement monogamy in the discrete analogue of analog Grover search, [arXiv:1611.04542](https://arxiv.org/abs/1611.04542).
- [25] H.-L. Shi, S.-Y. Liu, X.-H. Wang, W.-L. Yang, Z.-Y. Yang, and H. Fan, Coherence depletion in the Grover quantum search algorithm, *Phys. Rev. A* **95**, 032307 (2017).
- [26] Y.-C. Liu, J. Shang, and X. Zhang, Coherence depletion in quantum algorithms, *Entropy* **21**, 260 (2019).
- [27] S. Shubhalakshmi and U. Sen, Noncommutative coherence and quantum phase estimation algorithm, [arXiv:2004.01419](https://arxiv.org/abs/2004.01419).
- [28] C. Xiong and J. Wu, Geometric coherence and quantum state discrimination, *J. Phys. A: Math. Theor.* **51**, 414005 (2018).
- [29] S. Kim, L. Li, A. Kumar, C. Xiong, S. Das, U. Sen, A. K. Pati, and J. Wu, Protocol for unambiguous quantum state discrimination using quantum coherence, *Quantum Inf. Comput.* **21**, 931 (2021).
- [30] P. Zanardi, Entanglement of quantum evolutions, *Phys. Rev. A* **63**, 040304(R) (2001).
- [31] B. Kraus and J. I. Cirac, Optimal creation of entanglement using a two-qubit gate, *Phys. Rev. A* **63**, 062309 (2001).
- [32] F. Verstraete, K. Audenaert, and B. De Moor, Maximally entangled mixed states of two qubits, *Phys. Rev. A* **64**, 012316 (2001).
- [33] K. Życzkowski, P. Horodecki, M. Horodecki, and R. Horodecki, Dynamics of quantum entanglement, *Phys. Rev. A* **65**, 012101 (2001).

- [34] M. S. Leifer, L. Henderson, and N. Linden, Optimal entanglement generation from quantum operations, *Phys. Rev. A* **67**, 012306 (2003).
- [35] X. Wang, B. C. Sanders, and D. W. Berry, Entangling power and operator entanglement in qudit systems, *Phys. Rev. A* **67**, 042323 (2003).
- [36] P. J. Dodd and J. J. Halliwell, Disentanglement and decoherence by open system dynamics, *Phys. Rev. A* **69**, 052105 (2004).
- [37] A. R. R. Carvalho, F. Mintert, and A. Buchleitner, Decoherence and Multipartite Entanglement, *Phys. Rev. Lett.* **93**, 230501 (2004).
- [38] W. Dür and H.-J. Briegel, Stability of Macroscopic Entanglement under Decoherence, *Phys. Rev. Lett.* **92**, 180403 (2004).
- [39] M. P. Almeida, F. De Melo, M. Hor-Meyll, A. Salles, S. P. Walborn, P. H. Souto Ribeiro, and L. Davidovich, Environment-induced sudden death of entanglement, *Science* **316**, 579 (2007).
- [40] A. R. R. Carvalho, M. Busse, O. Brodier, C. Viviescas, and A. Buchleitner, Optimal Dynamical Characterization of Entanglement, *Phys. Rev. Lett.* **98**, 190501 (2007).
- [41] H. Bao-Lin and D. Yao-Min, Entanglement capacity of two-qubit unitary operator with the help of auxiliary system, *Commun. Theor. Phys.* **47**, 1029 (2007).
- [42] T. Konrad, F. de Melo, M. Tiersch, C. Kasztelan, A. Aragão, and A. Buchleitner, Evolution equation for quantum entanglement, *Nat. Phys.* **4**, 99 (2008).
- [43] S. M. Cohen, All maximally entangling unitary operators, *Phys. Rev. A* **84**, 052308 (2011).
- [44] C. H. Bennett, A. W. Harrow, D. W. Leung, and J. A. Smolin, On the capacities of bipartite Hamiltonians and unitary gates, *IEEE Trans. Inf. Theory* **49**, 1895 (2003).
- [45] F. Fröwis, Kind of entanglement that speeds up quantum evolution, *Phys. Rev. A* **85**, 052127 (2012).
- [46] A. Cheffles, Entangling capacity and distinguishability of two-qubit unitary operators, *Phys. Rev. A* **72**, 042332 (2005).
- [47] S. Ishizaka and T. Hiroshima, Maximally entangled mixed states under nonlocal unitary operations in two qubits, *Phys. Rev. A* **62**, 022310 (2000).
- [48] J. Batle, A. R. Plastino, M. Casas, and A. Plastino, On the distribution of entanglement changes produced by unitary operations, *Phys. Lett. A* **307**, 253 (2003).
- [49] M.-Y. Ye, D. Sun, Y.-S. Zhang, and G.-C. Guo, Entanglement-changing power of two-qubit unitary operations, *Phys. Rev. A* **70**, 022326 (2004).
- [50] X. Wang and P. Zanardi, Quantum entanglement of unitary operators on bipartite systems, *Phys. Rev. A* **66**, 044303 (2002).
- [51] J. Oppenheim, K. Horodecki, M. Horodecki, P. Horodecki, and R. Horodecki, Mutually exclusive aspects of information carried by physical systems: Complementarity between local and nonlocal information, *Phys. Rev. A* **68**, 022307 (2003).
- [52] J. K. Asbóth, J. Calsamiglia, and H. Ritsch, Computable Measure of Nonclassicality for Light, *Phys. Rev. Lett.* **94**, 173602 (2005).
- [53] Y. Yao, X. Xiao, L. Ge, and C. P. Sun, Quantum coherence in multipartite systems, *Phys. Rev. A* **92**, 022112 (2015).
- [54] A. Streltsov, U. Singh, H. S. Dhar, M. N. Bera, and G. Adesso, Measuring Quantum Coherence with Entanglement, *Phys. Rev. Lett.* **115**, 020403 (2015).
- [55] Z. Xi, Y. Li, and H. Fan, Quantum coherence and correlations in quantum system, *Sci. Rep.* **5**, 10922 (2015).
- [56] E. Chitambar and M.-H. Hsieh, Relating the Resource Theories of Entanglement and Quantum Coherence, *Phys. Rev. Lett.* **117**, 020402 (2016).
- [57] N. Killoran, F. E. S. Steinhoff, and M. B. Plenio, Converting Nonclassicality into Entanglement, *Phys. Rev. Lett.* **116**, 080402 (2016).
- [58] A. Streltsov, E. Chitambar, S. Rana, M. N. Bera, A. Winter, and M. Lewenstein, Entanglement and Coherence in Quantum State Merging, *Phys. Rev. Lett.* **116**, 240405 (2016).
- [59] X. Qi, T. Gao, and F. Yan, Measuring coherence with entanglement concurrence, *J. Phys. A: Math. Theor.* **50**, 285301 (2017).
- [60] H. Zhu, Z. Ma, Z. Cao, S.-M. Fei, and V. Vedral, Operational one-to-one mapping between coherence and entanglement measures, *Phys. Rev. A* **96**, 032316 (2017).
- [61] S. Chin, Coherence number as a discrete quantum resource, *Phys. Rev. A* **96**, 042336 (2017).
- [62] H. Zhu, M. Hayashi, and L. Chen, Axiomatic and operational connections between the  $l_1$ -norm of coherence and negativity, *Phys. Rev. A* **97**, 022342 (2018).
- [63] D. Egloff, J. M. Matera, T. Theurer, and M. B. Plenio, Of Local Operations and Physical Wires, *Phys. Rev. X* **8**, 031005 (2018).
- [64] L. Kraemer and L. del Rio, Currencies in resource theories, *Entropy* **23**, 755 (2021).
- [65] A. Mekala and U. Sen, All entangled states are quantum coherent with locally distinguishable pointers, *Phys. Rev. A* **104**, L050402 (2021).
- [66] K. Bu, A. Kumar, and J. Wu, Bell-type inequality in quantum coherence theory as an entanglement witness, [arXiv:1603.06322](https://arxiv.org/abs/1603.06322).
- [67] L. Qiu, Z. Liu, and F. Pan, Tripartite Bell-type inequalities for measures of quantum coherence and skew information, *Int. J. Quantum Inf.* **15**, 1750025 (2017).
- [68] D. Mondal, T. Pramanik, and A. K. Pati, Nonlocal advantage of quantum coherence, *Phys. Rev. A* **95**, 010301(R) (2017).
- [69] T. Chanda and S. Bhattacharya, Delineating incoherent non-Markovian dynamics using quantum coherence, *Ann. Phys.* **366**, 1 (2016).
- [70] S. Bhattacharya, S. Banerjee, and A. K. Pati, Evolution of coherence and non-classicality under global environmental interaction, *Quantum Inf. Process.* **17**, 236 (2018).
- [71] Z. Huang and H. Situ, Optimal protection of quantum coherence in noisy environment, *Int. J. Theor. Phys.* **56**, 503 (2017).
- [72] B. Çakmak, M. Pezzutto, M. Paternostro, and Ö. E. Müstecaplıoğlu, Non-Markovianity, coherence and system-environment correlations in a long-range collision model, *Phys. Rev. A* **96**, 022109 (2017).
- [73] C. Mukhopadhyay, S. Bhattacharya, A. Misra, and A. K. Pati, Dynamics and thermodynamics of a central spin immersed in a spin bath, *Phys. Rev. A* **96**, 052125 (2017).
- [74] A. Mortezaipoor, M. Ahmadi Borji, and R. Lo Franco, Non-Markovianity and coherence of a moving qubit inside a leaky cavity, *Open Syst. Inf. Dyn.* **24**, 1740006 (2017).
- [75] J. Ma, B. Yadin, D. Girolami, V. Vedral, and M. Gu, Converting Coherence to Quantum Correlations, *Phys. Rev. Lett.* **116**, 160407 (2016).

- [76] J. M. Matera, D. Egloff, N. Killoran, and M. B. Plenio, Coherent control of quantum systems as a resource theory, *Quantum Sci. Technol.* **1**, 01LT01 (2016).
- [77] Y. Guo and S. Goswami, Discordlike correlation of bipartite coherence, *Phys. Rev. A* **95**, 062340 (2017).
- [78] D. W. Berry and B. C. Sanders, Relation between classical communication capacity and entanglement capability for two-qubit unitary operations, *Phys. Rev. A* **68**, 032312 (2003).
- [79] A. Misra, U. Singh, S. Bhattacharya, and A. K. Pati, Energy cost of creating quantum coherence, *Phys. Rev. A* **93**, 052335 (2016).
- [80] L. Zhang, Z. Ma, Z. Chen, and S. M. Fei, Coherence generating power of unitary transformations via probabilistic average, *Quantum Inf. Process.* **17**, 186 (2018).
- [81] G. Styliaris, L. Campos Venuti, and P. Zanardi, Coherence-generating power of quantum dephasing processes, *Phys. Rev. A* **97**, 032304 (2018).
- [82] C. H. Bennett, D. P. DiVincenzo, J. A. Smolin, and W. K. Wootters, Mixed state entanglement and quantum error correction, *Phys. Rev. A* **54**, 3824 (1996).
- [83] E. M. Rains, Rigorous treatment of distillable entanglement, *Phys. Rev. A* **60**, 173 (1999).
- [84] P. M. Hayden, M. Horodecki, and B. M. Terhal, The asymptotic entanglement cost of preparing a quantum state, *J. Phys. A: Math. Gen.* **34**, 6891 (2001).
- [85] C. H. Bennett, H. J. Bernstein, S. Popescu, and B. Schumacher, Concentrating partial entanglement by local operations, *Phys. Rev. A* **53**, 2046 (1996).
- [86] M. A. Nielsen, Conditions for a Class of Entanglement Transformations, *Phys. Rev. Lett.* **83**, 436 (1999).
- [87] G. Vidal, Entanglement of Pure States for a Single Copy, *Phys. Rev. Lett.* **83**, 1046 (1999).
- [88] L. Hardy, Method of areas for manipulating the entanglement properties of one copy of a two-particle pure entangled state, *Phys. Rev. A* **60**, 1912 (1999).
- [89] D. Jonathan and M. B. Plenio, Minimal Conditions for Local Pure-State Entanglement Manipulation, *Phys. Rev. Lett.* **83**, 1455 (1999); **84**, 4781(E) (2000).
- [90] G. Vidal, Entanglement monotones, *J. Mod. Opt.* **47**, 2000 (2009).
- [91] K. Ben Dana, M. García Díaz, M. Mejatty, and A. Winter, Resource theory of coherence: Beyond states, *Phys. Rev. A* **95**, 062327 (2017).
- [92] J. Walgate and L. Hardy, Nonlocality, Asymmetry, and Distinguishing Bipartite States, *Phys. Rev. Lett.* **89**, 147901 (2002).
- [93] N. Khaneja and S. Glaser, Cartan decomposition of  $SU(2^n)$ , constructive controllability of spin systems and universal quantum computing, [arXiv:quant-ph/0010100](https://arxiv.org/abs/quant-ph/0010100).
- [94] S. A. Hill and W. K. Wootters, Entanglement of a Pair of Quantum Bits, *Phys. Rev. Lett.* **78**, 5022 (1997).
- [95] W. K. Wootters, Entanglement of Formation of an Arbitrary State of Two Qubits, *Phys. Rev. Lett.* **80**, 2245 (1998).
- [96] S. G. Johnson, The NLOpt nonlinear-optimization package, [http://github.com/stevengj/nlopt](https://github.com/stevengj/nlopt)
- [97] J. M. Gablonsky and C. T. Kelley, A locally-biased form of the DIRECT algorithm, *J. Global Optim.* **21**, 27 (2001).
- [98] T. P. Runarsson and X. Yao, Search biases in constrained evolutionary optimization, *IEEE Trans. Syst. Man Cybern. C* **35**, 233 (2005).
- [99] M. Ozols, How to generate a random unitary matrix, available at <http://home.lu.lv/~sd20008/papers/essays/Random>.
- [100] D. M. Bates and D. G. Watts, *Nonlinear Regression Analysis and Its Applications* (Wiley, New York, 1988); W. H. Press, S. A. Teukolsky, W. T. Vetterling, and B. P. Flannery, *Numerical Recipes: The Art of Scientific Computing* (Cambridge University Press, Cambridge, 2007); A. Sehwat, C. Srivastava, and U. Sen, Dynamical phase transitions in the fully connected quantum Ising model: Time period and critical time, *Phys. Rev. B* **104**, 085105 (2021).
- [101] C. Sanderson and R. Curtin, Armadillo: A template-based C++ library for linear algebra, *J. Open Source Software* **1**, 26 (2016).
- [102] C. Sanderson and R. Curtin, *Lecture Notes Comput. Sci.* **10931**, 422 (2018).
- [103] M. J. D. Powell, Direct search algorithms for optimization calculations, *Acta Numer.* **7**, 287 (1998).
- [104] T. Chanda, QIClib, <https://titaschanda.github.io/QIClib>.